Chapter 29. Cargo transport and asymmetric partitioning around curved surface boundaries: flat sheets, segmented tubes and terminal parasegments.

The succession of embryonic parasegmental fates is allocated with respect to the maternal Cad and Bcd gradients established in the oocyte, while formation of the D/V (L/R) axis is dependent the early zygotic transcription of WntD and the Tl signalling pathway. Both MyoII flux and the convergent-extension movements of gastrulation are constrained by embryonic surface topography. Meanwhile, cargo transport and preferential microtubule orientation, may be regulated via En and Wg, as core components of the segmentation cascade. During later development, the proliferative growth of the larval imaginal discs is predominantly asynchronous, with uncoupled cell-cycle progression in most cells. However, the fate of imaginal disc cells remains indeterminate until terminal PCP signalling, with the fine-scale patterning of adult tissues, and the assignment of differentiated cell fate, taking place during pupal metamorphosis. Many of the early embryonic functions are re-deployed throughout development, with their associated mutant phenotypes being dependant on the stage at which their wild-type functions are disrupted.

During the mid-blastoderm transition, P compartmental fate is allocated by *wg* and *en*; while A fate is specified by *wg* and *distal-less* (*dll*) [1]. Meanwhile, lack of the Hth Hox cofactor blocks the A > P succession of thoracic fates. The Hth and Exd cofactors may select between leg and wing fate; while Ey is expressed in eye-antennal and wing discs [2 3 4]. Over-expression of *Antp* deletes the eye-antennal disc, via *zen1-zen2*; while lack of *Antp* induces ectopic eyes in the wing [5 6]. However, somatic clones of homoeotic mutants may switch parasegmental fates autonomously, even when induced late in larval growth. In the wing disc, Dpp (TGFβ) promotes Ap/Ba cell elongation, with apico-lateral localisation of Rho1 [7]. Dpp is imported from the peripodial membrane, before being trafficked through baso-lateral cell interfaces in MVBs [8 9 10 11]. Thus, the embryonic axial system is maintained during larval growth, although the Cartesian axes of twin-field boundary cells may be rotated. In particular, growth along the Pr/Dist axis of the wing blade is regulated via the rapid degradation of Dpp in the P compartment [7]. At the pre-pupal stage, the marginal (D/V) loop and Pr/Dist ring of Wg expression intersect each other near the presumptive hinge region. Thus, the wing disc is divided into four quadrants, with an A/P AMS on both presumptive surfaces of the blade. At the wing tip, the D/V margin intersects the A/P compartment boundary at 90º, and further growth is inhibited; consistent with a block in Wg uptake through the Ap disc surface. In this distal region, the hairs remain aligned with the Pr > Dist axis of the wing blade, rather than the D/V margin. Notably, the Distal-less (Dll) Hox co-factor is expressed around the D/V margin, the presumptive veins and in the wing tip (distal to V2 and V5) [12]. Phosphorylation of a Zif/Dll complex may also regulate the asymmetric expression of aPKC and Miranda [13].

By contrast, the rows of bristles in the notum are aligned along the A > P embryonic axis. By this criterion, the long axis of the wing blade is rotated through 90º in the central region of the disc during metamorphosis. Notably, the A intersection of the Pr/Dist Wg ring and D/V loop of Wg expression may act as site for homoeotic tarsal outgrowths, see [14]. Meanwhile, the fate of the hinge region is specified by the Spalt complex TFs: *spalt-related* (*salr*), *spalt major* (*salm*) and *spalt adjacent* (*sala*) [15 16 17 18]. Within the wing blade, *salm* regulates inter-vein growth, while the delivery of Dpp is suppressed by Wg [19 20 16]. The presumptive long veins disc run parallel to the A/P compartment boundary and orthogonal to the cross-veins [21 22] (Fig. 46A). It is only during pupal metamorphosis that the shape of the wing blade is remodelled, with compaction of the hinge region. In consequence, the adult longitudinal veins converge near the hinge, while their distal tips spread out around the D/V margin. Thus, the wing veins may act like late-forming twin-field boundaries during the passage of a Pr > Dist morphogenetic wave. These interactions are regulated via TGFβ

growth factor signalling, with the Rho^{ve} protease *veinlet*, being expressed around the D/V wing margin and presumptive veins.

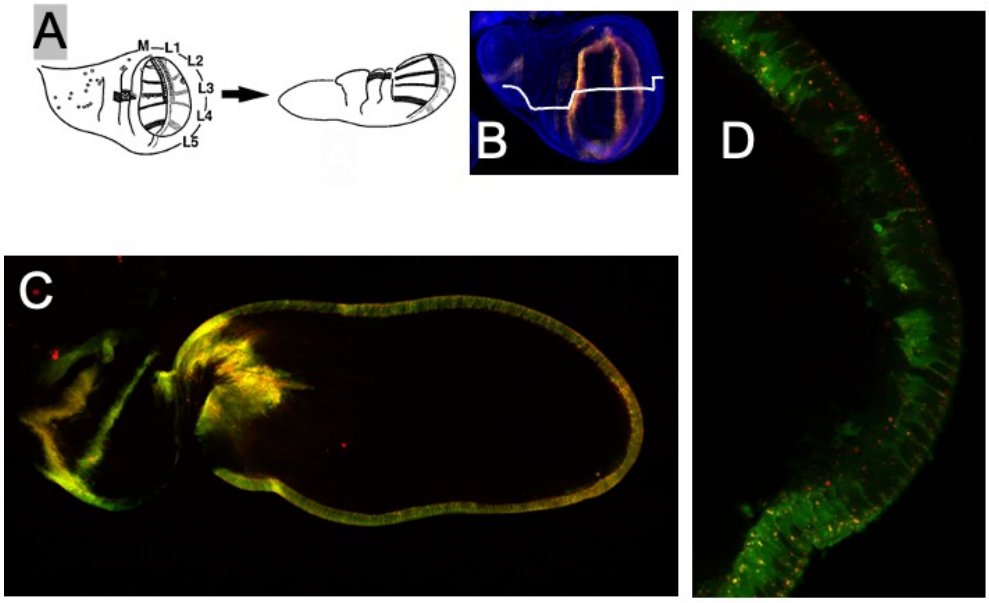

Fig. 45. Eversion of the imaginal wing disc. A. In the L3 disc, the presumptive long veins (L2-L5) are roughly parallel to the A/P boundary, with V1 running along the anterior D/V margin, reproduced from Sturtevant and Bier 1995. **B.** Confocal image *wg-Gal4; UAS-GFP-mCD8-mCherry* L3 disc. The Pr ring of *wg-Gal4* expression marks the hinge/blade boundary, with a Pr/Dist loop around the D/V margin (yellow/red), background Dapi (blue) marks nuclei in the focal plane around edge of the disc, white line indicates position of A/P boundary crossing wing blade and notum. **C.** Everted disc from mature pupa: *wg-Gal4*; *UAS-GFP-mCD8-mCherry*. The *wg-Gal4* expressing cells along the D/V margin (yellow/green /red) are trapezoidal, consistent with axial rotations of these cells around the edge of the wing blade. These marginal cells may constrain the shape of the wing blade. Gubb and Gurrero, unpublished. **D.** Distal tip of pupal wing blade: *wg-Gal4*; *UAS-GFP-mCD8-mCherry*. Ap/Ba orientation of marginal cells appears orthogonal to the plane of the wing blade. The GFP fluor may be partially suppressed in putative MVBs (bright red punctae).

Notably, regulatory mutations of embryonic functions may affect the shape and venation pattern of the wing [23]. In particular, amorphic mutations in the 5' regulatory region of the gap gene *kni^{ri}* (*radius incompletus*) delete the entire V2; while hypomorphic *kni^{ri}* alleles remove only its distal tip (Lindsley and Zimm 1992) [24] [14]. Similarly, hypomorphic *cubitus interruptus* (*ci*) alleles delete the proximal cross-vein, while amorphic *ci* alleles alter the wing shape and venation pattern, via the Hh signalling pathway. Mutants of the segmentation gene *hairy* show ectopic bristles along the wing veins, and on other parts of the body surface [25]. By contrast, viable *gt* mutants extend the larval growth phase, and increase the size of adult flies; consistent with partial insensitivity to ecdysone signalling [26]. Thus, the morphogenetic functions that determine regional fate during embryogenesis may be re-deployed, with mutant phenotypes that reflect later functions during terminal differentiation.

Towards the end of larval growth, the presumptive vein cells become more compact than surrounding intervein cells, before hexagonal tessellation during the pupal stage [27] [28]. The Wg expressing cells along the D/V margin, however, become trapezoidal; consistent with

axial rotations in the epithelial plane (Fig. 45). Thus, the Pr > Dist morphogenetic waves may re-align cell interfaces, and canalise morphogen flux, as the pupal wing blade is remodelled. Occasional rosette cell clusters form sensory organ precursors (SOPs) along the anterior D/V margin and veins, giving rise to innervated bristles and campaniform sensillae. Notably, the ectopic bristles in *hairy* and *Hairy wing* mutants have the same orientation as surrounding wing hairs, in both wild-type and PCP mutant backgrounds [29]. In notal bristle-forming SOPs, Par3, Mir and Numb are trafficked along the mitotic spindle; with asymmetric partitioning of Numb and N between daughter cells as they adopt differential (M-twin) fates [30 31]. In the absence of Par6, neuroblast spindles become misoriented, the Ap localisation of Par3 (Baz) fails and the Ba localisation of Numb and Miranda is blocked [31]. Thus, asymmetrical partitioning of Par/Cdc42 couples the spindle axes of dividing cells and may displace all three Cartesian axes during terminal PCP signalling. On the Ap epithelial surface, the Fz, Wg signal-receptor, and the Stan, transmembrane cadherin, interact with Par3 (Baz) [32 33]. Meanwhile, Vang localises to the anterior SOP daughter cell as Baz is distributed in a P crescent [34]. In all these interactions, the distribution of Baz may be linked to the asymmetric localisation of Centrosomin, see [35].

In transgenic *ap-Gal4; UAS-Dll*, the misexpression of Dll may induce growth of homoeotic tarsal outgrowths from the anterior D/V margin near the A hinge; while the distal tip of the haltere may transform to T5, with pre-tarsal claws [12]. In these regions, altered Wg flux may switch between D and V disc fates. However, overexpression of *UAS-pk^{sple}* in the D wing (in *ap-Gal4; UAS-pk^{sple}* flies) reverses bristle polarity along the D margin, without affecting adjacent bristles on the V surface, which retain their wild-type orientation (Fig. 22). By implication, alterations in Wg flux may not be transmitted across the N/Delta interface along the D/V margin. However, overexpression of *UAS-pk^{sple}* along the presumptive veins (in *Dll-Gal4; UAS-pk^{sple}* wings) gives a PCP pattern, like that of *pk^{pk}* mutants (Fig. 46).

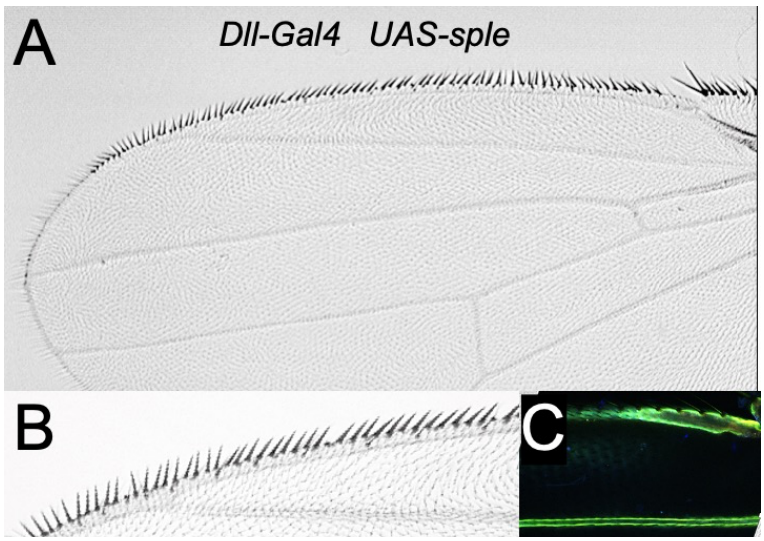

Fig. 46. Overexpression of the Pk^{sple} isoform along wing veins in *dll-Gal4; UAS-pk^{sple}* wing. **A.** and **B.** Phase contrast wing blade, showing PCP pattern similar to *pk^{pk}*, consistent with altered Wg flux during terminal PCP signalling. **C.** *Dll-Gal4* expression in adult wing, confocal image of adult wing (V1/V2): *Dll-Gal4*; *UAS-GFP-mCD8-mCherry*.

The expression of Delta in wild-type L3 discs is restricted to the presumptive veins, while N and Pk are expressed in the inter-veins regions [36 37]. By these criteria, the wing veins may represent late-forming field boundaries. By contrast, overexpression of the *Pk^{sple}* isoform (in *da-Gal4; UAS-pk^{sple}* flies) gives altered bristle polarity along the anterior D/V margin; with

topological disclinations in hairs, at variable positions within the wing blade 37 (Fig. 5E). Such alterations in planar polarity are also dependent on the Ap/Ba epithelial axis, as overexpression of Baz (Par3) in somatic mosaics alters the Ap/Ba localisation of Stan, with domineering PCP alterations in surrounding wild-type cells [33]

The organisation of the leg discs is similar to that of the wing in that the peripheral regions give rise to notum, followed by proximal leg segments, with the tarsal segments (T1-T5) being delineated by concentric rings towards the disc centre [14]. In this system, Distalless (Dll) selects the central, tarsal, fates via the Wg and Dpp signalling pathways [38 39 40]. Disc eversion is driven primarily via actomyosin contractions in the peripodial membrane; which may require proteolytic degradation of the extracellular matrix [41 42 43]. The infolding cells at tarsal segmental boundaries become cuboidal [44]. Growth of the central disc region may be regulated via the Ft/Ds/Fj cassette, by the criterion that the middle (T2/T3) segmental joint is lost in *fj* mutants [45 46]. During normal development, the expression of a ring of *ap* in T4 may restrict Wg transmission to the distal limb tip, see [47]. The concentric rings of *wg* transcription at tarsal segmental boundaries may be co-incident with N expression, with Wg trafficked through lateral cell interfaces, in either direction along the Pr/Dist limb axis. The critical role of the N is also apparent in somatic *N* clones, which induce foreshortened limbs, lacking segmental boundaries, with T1 fused to the T5 pre-tarsus, see [48]. By contrast, reduced Wg uptake through the Ap epithelial surface may halve the length of each tarsal segment in PCP mutants, generating ectopic AMSs with mirror-image joints in T1 to T4, (Fig. 47), see [49]. However, the Dist T5 remains unaffected, consistent with a lack of Ap Wg uptake in the centre of the disc during normal development. Wg transport between lateral cell interfaces may continue in the pre-tarsus, with twin-field rotation to terminate the chain of parasegments, replacing a Dist joint structure with tarsal claws.

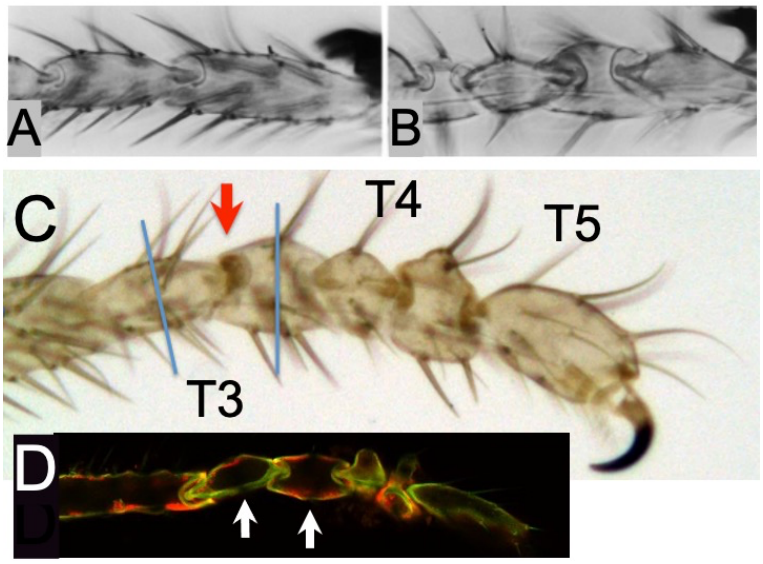

Fig. 47. Tarsal leg segments. A. wild-type. **B.** pk^{sple1}. **C.** pk^{sple1} ectopic segmental boundary in T3 (red arrow), with double (Pr and Dist) AMSs (blue lines), phase contrast. **D.** Confocal image pk^{sple} tarsal segments *pk-GFP* green; *E-Cad-TFP* red, $pk^{Mi(MIC)7065\text{-}GFP}/pk^{sple1}$; *E-Cad-TFP*. The *E-Cad-TFP* Teal fluor signal is shown in red, Gubb and Reichhart, unpublished. White arrows indicate putative ectopic Pr and Dist AMSs in the T3 segment.

At the transcriptional level, the T5 pre-tarsal joint is delimited by *Fascilin-2* (Fas-2) expression, with terminal TFs expression including *aristaless*, *B*, *Dll*, *clawless*, *tarsalless*, *ap* and *LIM1* [50 51 52 53 54 55]. In addition, the Zn-finger TFs Odd, Sop, Drm and Bowl are

expressed at tarsal segmental boundaries, and within the pre-tarsus; with the Homeobox TFs acting through Groucho [56 57 58]. In conjunction, these morphogenetic functions may block the formation of a terminal T5 joint and substitute the alternative pathway that terminates limb growth. Strikingly, the pre-tarsus develops a terminal infolding along the A/P boundary, separating mirror-image tarsal claws [44 59]. By implication, an axial rotation takes place around the Pr/Dist AMS of T5, Fig. 48. On this interpretation, the Dist tip of the A/P compartment infolds as a radial segmental boundary, with a 90^{o} rotation of Cartesian axes and mirror twin tarsal claws. Overexpression of activated Notch* (or Odd) along the A/P boundary induces a deep radial groove near the disc centre, in *ptc-Gal4; UAS-N**, or *ptc-Gal4; UAS-odd* larvae [57].

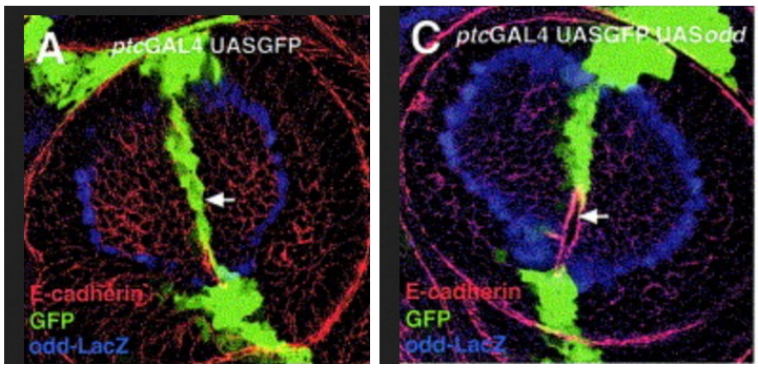

Fig. 48. Ectopic ectopic expression of Odd (or activated Notch*) disrupts formation of pre-tarsal fold in the T5 of *ptc-Gal4; UAS-N**, or *ptc-Gal4; UAS-odd* leg discs. **A.** *ptc-Gal4* is expressed in a narrow (green) ribbon just anterior to the A/P boundary, white arrow. E-Cad localisation at cell interfaces (red) is increased at tarsal segmental boundaries. **B.** Ectopic expression of Odd along the A/P boundary in the central disc converts the putative radial AMS into a deep furrow between pre-tarsal twin-fields. From Natori et al., 2012.

These coordinated alterations in TF activity are consistent with reduced Ap Wg import with residual Wg flux in terminal parasegments, without an extracellular Wg gradient being formed, see [59].

The polarity of abdominal bristles is also aligned with respect to A/P compartmental boundaries, with occasional SOP rosettes recruited from the surrounding interstitial cells [60]. As the migrating histoblasts meet during the pupal stage an irregular interface is formed between A and P cell populations. Actomyosin cables are coupled through lateral cell interfaces (D/V, L/R) with pulsatile contractions causing progressive straightening of the A/P boundary [60]. The alignment of heterotypic interfaces at the A/P boundary gradually spreads outwards to give a sheet of elongated, parallel-sided cells, with homotypic (A/A and P/P) interfaces. As during gastrulation, this epithelial remodelling is dependent on *Tl* and *en,* although with the parallel-side cells are aligned with respect to D/V (L/R), rather than the A/P axis, of the abdomen. The Dachs (D) myosin anchor is localised preferentially to the P interface of A cells, and the A interface of P cells [61 62 63]. Taken together, these results confirm the critical role of contractile shortening of matrix-coupled actomyosin cables in driving the realignment of cellular interfaces.

During larval growth, epithelial cells are free-cycling and intercalate with neighbouring cells as they divide. In general, disc cells show salt-and-pepper expression of cyclin-dependent fluors, except for G_1 arrest at the D/V boundary, in the wing disc, and along the advancing morphogenetic furrow, in the eye-antennal disc. Notably, the A/P boundary in the wing and the perimeter of the eye twin-field are not apparent [64 65]. By contrast, during terminal PCP signalling Pr/Dist morphogenetic waves aligns cellular interfaces and regulates asymmetrical partitioning. These coordinated changes deploy cell-cycle dependent regulation

of actin microfilaments and the microtubule cytoskeleton. Cytoskeletal remodelling may drive axial rotations around Ap/Ba epithelial axis, or in the epithelial plane. However, rotation around any one Cartesian axis must displace the other two (Fig. 28), with differential Ap/Ba trafficking to either side of AMSs. Thus, morphogenetic twin-fields may adopt differential fates during normal development, or a mutant patch of cells may be allocated an alternative fate during larval growth. In this sense, differentiated cell fate, and fine-scale tissue patterning, are set without reference to a global positional information matrix.

Summary:

Cytoplasmic remodelling regulates the alignment of cellular interfaces and the surface topography of epithelial sheets, with altered mitotic spindle orientations, asymmetric partitioning of TFs, and canalised morphogen flux. These constraints are relatively loose during the proliferative growth of imaginal discs; but become critical during terminal PCP signalling. Most larval disc cells are free-cycling, with G_1 arrest at twin-field boundaries. In general, the embryonic axes are maintained, but may be rotated in the centre of imaginal discs with tubular limb outgrowths. In this context, the tarsal segmental joints may represent late-forming twin-field boundaries, consistent with a harmonic standing wave along the Pr/Dist limb axis. The growth of the T5 pre-tarsus and the tip of the wing blade may be supressed by a block in Wg import through the Ap epithelial surface. Similarly, PCP mutants may halve the length, and double the number, of the T1-T4 segments. Metachronal waves of contraction drive the alignment of cytoplasmic interfaces within SOP rosettes and their surrounding interstitial cells. In this sense, the allocation of differentiated cell fate does not require a global positional information matrix. The region-specific patterns of TF expression may be maintained in adult tissues, as the metabolic range of individual cells is restricted.

References:

1. Simcox, A. A. *et al.* Imaginal discs can be recovered from cultured embryos mutant for the segment-polarity genes engrailed naked and patched but not from wingless. *Development* **107**, 715–722 (1989).
2. Casares, F. & Mann, R. S. Control of antennal versus leg development in Drosophila. *Nature* **392**, 723 (1998).
3. Noro, B., Culi, J., McKay, D. J., Zhang, W. & Mann, R. S. Distinct functions of homeodomain-containing and homeodomain-less isoforms encoded by homothorax. *Genes Dev.* **20**, 1636–1650 (2006).
4. Abu-Shaar, M. & Mann, R. S. Generation of multiple antagonistic domains along the proximodistal axis during Drosophila leg development. *Development* **125**, 3821 (1998).
5. Plaza, S. *et al.* Molecular basis for the inhibition of Drosophila eye development by Antennapedia. *EMBO J.* **20**, 802–811 (2001).
6. Beh, C. Y. *et al.* Roles of cofactors and chromatin accessibility in Hox protein target specificity. *Epigenetics Chromatin* **9**, 1 (2016).
7. Widmann, T. J. & Dahmann, C. Dpp signaling promotes the cuboidal-to-columnar shape transition of Drosophila wing disc epithelia by regulating Rho1. *J. Cell Sci.* **122**, 1362–1373 (2009).
8. Gibson, M. C., Lehman, D. A. & Schubiger, Gerold, G. Lumenal transmission of Decapentaplegic in Drosophila imaginal discs. *Dev. Cell* **3**, 451–460 (2002).

9. Valentine, Hogan Justin, & Collier Simon. The Drosophila Chmp1 protein determines wing cell fate through regulation of epidermal growth factor receptor signaling. *Dev. Dyn.* **243**, 977–987 (2014).
10. Tjota, M. *et al.* Annexin B9 binds to {beta}H-spectrin and is required for multivesicular body function in Drosophila. *J. Cell Sci.* **124**, 2914–2926 (2011).
11. Harmansa, S., Hamaratoglu, F., Affolter, M. & Caussinus, E. Dpp spreading is required for medial but not for lateral wing disc growth. *Nature* **527**, 317 (2015).
12. Gorfinkiel, N., Morata, G. & Guerrero, I. The homeobox gene Distal-less induces ventral appendage development in Drosophila. *Genes Dev.* **11**, 2259–2271 (1997).
13. Chang, K. C. *et al.* Interplay between the transcription factor Zif and aPKC regulates neuroblast polarity and self-renewal. *Dev. Cell* **19**, 778–785 (2010).
14. Held, L. I. *Imaginal Discs: The Genetic and Cellular Logic of Pattern Formation*. (Cambridge University Press, 2002).
15. de Celis, J. F., Barrio, R. & Kafatos, F. C. A gene complex acting downstream of dpp in Drosophila wing morphogenesis. *Nature* **381**, 421–424 (1996).
16. Barrio, R., de Celis, J. F., Bolshakov, S. & Kafatos, F. C. Identification of regulatory regions driving the expression of the Drosophila spalt complex at different developmental stages. *Dev. Biol.* **215**, 33–47 (1999).
17. Organista, M. F. *et al.* The Spalt transcription factors generate the transcriptional landscape of the Drosophila melanogaster wing pouch central region. *PLoS Genet.* **11**, e1005370 (2015).
18. Baëza, M. *et al.* Inhibitory activities of short linear motifs underlie Hox interactome specificity in vivo. *eLife* **4**, e06034 (2015).
19. Baena-López, L. A., Pastor-Pareja, J. C. & Resino, J. Wg and Egfr signalling antagonise the development of the peripodial epithelium in Drosophila wing discs. *Development* **130**, 6497 (2003).
20. Akiyama, T. *et al.* Dally regulates Dpp morphogen gradient formation by stabilizing Dpp on the cell surface. *Dev. Biol.* **313**, 408–419 (2008).
21. Sturtevant, M. A. & Bier, E. Analysis of the genetic hierarchy guiding wing vein development in Drosophila. *Dev. Camb. Engl.* **121**, 785–801 (1995).
22. Baena-López, L. A., Baonza, A. & García-Bellido, A. The orientation of cell divisions determines the shape of Drosophila organs. *Curr. Biol.* **15**, 1640–1644 (2005).
23. Diaz-Benjumea, F. J. & Garcia-Bellido, A. Genetic analysis of the wing vein pattern of Drosophila. *Rouxs Arch. Dev. Biol.* **198**, 336–354 (1990).
24. Lunde, K., Biehs, B., Nauber, U. & Bier, E. The knirps and knirps-related genes organize development of the second wing vein in Drosophila. *Development* **125**, 4145–4154 (1998).
25. Lindsley, D. L & Zimm, G. G. *The Genome of Drosophila Melanogaster.* (Academic press, 1992).
26. Simpson, P & Morata, G. Simpson, P., & Morata, G. (1980). The control of growth in the imaginal discs of Drosophila. (pp. 129-139). Springer, Boston, MA. *Dev. Neurobiol. Drosoph.* 129–139 (1980).
27. Baena-López, L. A., Baonza, A. & García-Bellido, A. The orientation of cell divisions determines the shape of Drosophila organs. *Curr. Biol.* **15**, 1640–1644 (2005).
28. Classen, A. K., Anderson, K. I., Marois, E. & Eaton, S. Hexagonal packing of Drosophila wing epithelial cells by the planar cell polarity pathway. *Dev. Cell* **9**, 805–817 (2005).
29. Gubb, D. & Garcia-Bellido, A. A genetic analysis of the determination of cuticular polarity during development in Drosophila melanogaster. *J. Embryol. Exp. Morphol.* **68**, 37–57 (1982).

30. Couturier, L., Mazouni, K. & Schweisguth, F. Numb localizes at endosomes and controls the endosomal sorting of notch after asymmetric division in Drosophila. *Curr. Biol.* **23**, 588–593 (2013).
31. Petronczki, M. & Knoblich, J. A. DmPAR-6 directs epithelial polarity and asymmetric cell division of neuroblasts in Drosophila. *Nat. Cell Biol.* **3**, 43 (2000).
32. Djiane, A., Yogev, S. & Mlodzik, M. The apical determinants aPKC and dPatj regulate Frizzled-dependent planar cell polarity in the Drosophila eye. *Cell* **121**, 621–631 (2005).
33. Wasserscheid, I., Thomas, U. & Knust, E. Isoform-specific interaction of Flamingo/Starry Night with excess Bazooka affects planar cell polarity in the Drosophila wing. *Dev. Dyn.* **236**, 1064–1071 (2007).
34. Bellaiche, Y., Gho, M., Kaltschmidt, J. A., Brand, A. H. & Schweisguth, F. Frizzled regulates localization of cell-fate determinants and mitotic spindle rotation during asymmetric cell division. *Nat Cell Biol* **3**, 50–57 (2001).
35. Chen, G., Rogers, A. K., League, G. P. & Nam, S. C. Genetic interaction of centrosomin and bazooka in apical domain regulation in Drosophila photoreceptor. *PLoS One* **6**, e16127 (2011).
36. de Celis, J. F., Bray, S. & Garcia-Bellido, A. Notch signalling regulates veinlet expression and establishes boundaries between veins and interveins in the Drosophila wing. *Development* **124**, 1919 (1997).
37. Gubb, D. *et al.* The balance between isoforms of the prickle LIM domain protein is critical for planar polarity in Drosophila imaginal discs. *Genes Dev.* **13**, 2315–2327 (1999).
38. Cohen, S. M. & Jurgens, G. Proximal-distal pattern formation in Drosophila: cell autonomous requirement for Distal-less gene activity in limb development. *EMBO J.* **8**, 2045–2055 (1989).
39. Galindo, M. I., Bishop, S. A., Greig, S. & Couso, J. P. Leg patterning driven by proximal-distal interactions and EGFR signaling. *Science* **297**, 256 (2002).
40. Galindo, M. I., Fernández-Garza, D., Phillips, R. & Couso, J. P. Control of Distal-less expression in the Drosophila appendages by functional 3' enhancers. *Dev. Biol.* **353**, 396–410 (2011).
41. Fristrom, D. K. The mechanism of evagination of imaginal discs of Drosophila melanogaster. *Dev. Biol.* **54**, 163–171 (1976).
42. Appel, L. F. *et al.* The Drosophila Stubble-stubbloid gene encodes an apparent transmembrane serine protease required for epithelial morphogenesis. *Proc. Natl. Acad. Sci. U. S. A.* **90**, 4937–4941 (1993).
43. Diaz-de-la-Loza, M.-D.-C., Loker, R., Mann, R. S. & Thompson, B. J. Control of tissue morphogenesis by the HOX gene *Ultrabithorax*. *Dev. Camb. Engl.* **147**, (2020).
44. Fristrom, D. K. The mechanism of evagination of imaginal discs of Drosophila melanogaster. *Dev. Biol.* **54**, 163–171 (1976).
45. Tokunaga, C. & Gerhart, J. C. The effect of growth and joint formation on bristle pattern in D. melanogaster. *J. Exp. Zool.* **198**, 79–95 (1976).
46. Villano, J. L. & Katz, F. N. four-jointed is required for intermediate growth in the proximal-distal axis in Drosophila. *Development* **121**, 2767–2777 (1995).
47. Fernandez-Funez, P., Lu, C. H., Rincon-Limas, D. E., Garcia-Bellido, A. & Botas, J. The relative expression amounts of apterous and its co-factor dLdb/Chip are critical for dorso-ventral compartmentalization in the Drosophila wing. *EMBO J.* **17**, 6846–6853 (1998).
48. de Celis, J. F., Tyler, D. M., de Celis, J. & Bray, S. J. Notch signalling mediates segmentation of the Drosophila leg. *Dev. Camb. Engl.* **125**, 4617–4626 (1998).

49. Held, L. I., Duarte, C. M. & Derakhshanian, K. Extra tarsal joints and abnormal cuticular polarities in various mutants of Drosophila melanogaster. *Rouxs Arch. Dev. Biol.* **195**, 145–157 (1986).
50. Pueyo, J. I. & Couso, J. P. Chip-mediated partnerships of the homeodomain proteins Bar and Aristaless with the LIM-HOM proteins Apterous and Lim1 regulate distal leg development. *Development* **131**, 3107 (2004).
51. Kojima, T., Tsuji, T. & Saigo, K. A concerted action of a paired-type homeobox gene, aristaless, and a homolog of Hox11/tlx homeobox gene, clawless, is essential for the distal tip development of the Drosophila leg. *Dev. Biol.* **279**, 434–445 (2005).
52. Sakurai, K. T., Kojima, T., Aigaki, T. & Hayashi, S. Differential control of cell affinity required for progression and refinement of cell boundary during Drosophila leg segmentation. *Dev. Biol.* **309**, 126–136 (2007).
53. Tajiri, R., Tsuji, T., Ueda, R., Saigo, K. & Kojima, T. Fate determination of Drosophila leg distal regions by trachealess and tango through repression and stimulation, respectively, of Bar homeobox gene expression in the future pretarsus and tarsus. *Dev. Biol.* **303**, 461–473 (2007).
54. Pueyo, J. I. & Couso, J. P. The 11-aminoacid long Tarsal-less peptides trigger a cell signal in Drosophila leg development. *Dev. Biol.* **324**, 192–201 (2008).
55. Miyazono, K. *et al.* Cooperative DNA-binding and sequence-recognition mechanism of aristaless and clawless. *EMBO J.* **29**, 1613–1623 (2010).
56. Hart, M. C., Wang, L. & Coulter, D. E. Comparison of the structure and expression of odd-skipped and two related genes that encode a new family of zinc finger proteins in Drosophila. *Genetics* **144**, 171–182 (1996).
57. Hao, I., Green, R. B., Dunaevsky, O., Lengyel, J. A. & Rauskolb, C. The odd-skipped family of zinc finger genes promotes Drosophila leg segmentation. *Dev. Biol.* **263**, 282–295 (2003).
58. Goldstein, R. E. *et al.* An eh1-like motif in odd-skipped mediates recruitment of Groucho and repression in vivo. *Mol. Cell. Biol.* **25**, 10711–10720 (2005).
59. Natori, K., Tajiri, R., Furukawa, S. & Kojima, T. Progressive tarsal patterning in the Drosophila by temporally dynamic regulation of transcription factor genes. *Dev. Biol.* **361**, 450–462 (2012).
60. Iijima, N., Sato, K., Kuranaga, E. & Umetsu, D. Differential cell adhesion implemented by Drosophila Toll corrects local distortions of the anterior-posterior compartment boundary. *Nat. Commun.* **11**, 6320 (2020).
61. Mao, Y. *et al.* Dachs: an unconventional myosin that functions downstream of Fat to regulate growth, affinity and gene expression in Drosophila. *Development* **133**, 2539–2551 (2006).
62. Mangione, F. & Martín-Blanco, E. The Dachsous/Fat/Four-jointed pathway directs the uniform axial orientation of epithelial cells in the Drosophila abdomen. *Cell Rep.* **25**, 2836-2850.e4 (2018).
63. Chorro, A. *et al.* Planar cell polarity: intracellular asymmetry and supracellular gradients of Dachsous. *Open Biol.* **12**, 220195 (2022).
64. O'Brochta, D. A. & Bryant, P. J. A zone of non-proliferating cells at a lineage restriction boundary in Drosophila. *Quinquenn. Rep. Dev. Biol. Cent. Univ. Calif. Irvine* 59–60 (1985).
65. Zielke, N. *et al.* Fly-FUCCI: a versatile tool for studying cell proliferation in complex tissues. *Cell Rep.* **7**, 588–598 (2015).